J. Electroanal. Chem., 171 (1984) 303–316
Elsevier Sequoia S.A., Lausanne – Printed in The Netherlands

CHANGES IN THE POLYCRYSTALLINE GOLD ELECTRODE SURFACE PRODUCED BY SQUARE WAVE POTENTIAL PERTURBATIONS

A.C. CHIALVO, W.E. TRIACA and A.J. ARVÍA

Instituto de Investigaciones Fisicoquímicas Teóricas y Aplicadas (INIFTA), Casilla de Correo 16, Sucursal 4, 1900 La Plata (Argentina)

(Received 19th May 1983; in revised form 15th February 1984)

ABSTRACT

The electroreduction of gold oxide layers produced by a square wave potential signal (SWPS) under a proper set of perturbation conditions yields a reproducible electrode surface with a large increase in the surface area. The different variables are systematically investigated to establish the optimal conditions of the SWPS. The results are discussed on the basis of the thermodynamics and kinetics of oxide monolayer and multilayer formation.

INTRODUCTION

The electrochemical behaviour of noble metal electrodes can be considerably modified by either mechanical, chemical or electrochemical treatments as is shown by their reproducibility, electrocatalytic activity and performance during a particular electrochemical process. The influence of the electrode pre-treatment on the rest potential and double layer capacitance of gold in aqueous solutions has been known for a long time [1].

On the other hand, thick oxide layers which can be formed on noble metal electrodes exhibit interesting charge storage responses [2], electrocatalytic properties towards reactions such as the oxygen evolution reaction [3–5], electrochromic behaviour [6] and electroreduction characteristics yielding fresh electrode surfaces involving, for some metals, a remarkable enhancement of electrochemical reaction rates [7]. These interesting features are observed for gold electrodes in both acid and base electrolytes [8,9].

The structure of the gold/aqueous electrolyte interface after anodizing either under stationary or non-stationary conditions becomes very complex, as concluded from optical measurements [10–12] and seems to depend to a great extent on the history of the electrode including the type of perturbation applied to it [13]. The activation of noble metals can be achieved starting from the initial anodic formation of a thick hydrous oxide layer, which upon electroreduction yields an electrode surface covered with a thin layer of the noble metal [14]. This procedure has been

0022-0728/84/$03.00

applied both under potential cycling [9] and under square wave potential cycling (SWPS) conditions [14].

The present work reports the surface area increase of gold electrodes in acid electrolytes achieved by the SWPS procedure. The latter, as it operates under constant potential conditions both at the upper and lower potential limits, should, in principle, facilitate both the interpretation of the oxide formation and the correlation of the corresponding potentials with bulk thermodynamic data.

The electroreduction of the anodic layer formed under SWPS conditions yields a very reproducible electrode surface with an increased surface area, as has already been observed in the case of platinum electrodes in acid electrolyte [14].

EXPERIMENTAL

Runs were made in a three electrode compartment Pyrex glass cell. Two types of gold (Johnson Matthey Co.) working electrode were used, either as wires (4–6 cm long and 0.5 mm diameter) or plates (2 × 6 mm). The working electrode was first electropolished with ac (50 Hz, 10–15 V) in 8 M H_2SO_4. Then, it was repeatedly rinsed with triply distilled water and finally immersed for 1 h in a solution similar to that used in the cell, to attain a reproducible surface electrode condition. The potentiodynamic behaviour of the treated electrodes in the 0.01–1.75 V range was very reproducible. A gold plate counterelectrode was used. The counterelectrode compartment was connected directly to the rest of the cell to minimize the ohmic drop between electrodes. Runs were made in $HClO_4$ solutions ($0.1\ M \leqslant c_{HClO_4} \leqslant 2\ M$) at 30 °C. A hydrogen reference electrode in the same acid electrolyte solution was employed.

The anodization procedure consisted of applying a square wave potential signal (SWPS) to the working electrode between lower ($0.0\ V \leqslant E_l \leqslant 2.7\ V$) and upper ($2.0\ V \leqslant E_u \leqslant 3.0\ V$) potential values at a certain frequency ($0.5\ kHz \leqslant f \leqslant 10\ kHz$) during a certain time (t). The duration of each potential step, τ_l and τ_u, respectively was adjusted at convenience. Most of the results reported in this paper correspond to $\tau_l = \tau_u$ except where otherwise stated. E_u was always located in the potential range where a thick gold oxide layer grows. Potentiodynamic electroreduction profiles of the thick gold oxide layer at 0.01 V/s were run immediately after the SWPS treatment.

The change in the real area of the working electrode produced by the SWPS treatment was determined by comparing the electroreduction charges of the oxide layers participating when the electrode is subjected to a repetitive triangular potential sweep (RTPS) at 0.1 V/s in the 0.05 V to 1.75 V range, before and after the SWPS treatment. The circuitry and further details of the experimental setup are the same as previously described [14]. X-ray diffractograms and SEM photographs of gold electrode surfaces resulting from different treatments were obtained.

RESULTS

(1) Voltamperometric characteristics of a gold electrode after applying the square wave potential signal

The base voltammogram run with an electropolished gold electrode in 1 *M* $HClO_4$ after 5 min RTPS at 0.1 V/s between 0.05 V and 1.75 V (Fig. 1a), exhibits the already known complex current peaks related to the electroformation and electroreduction of the gold oxide layer. When the gold electrode is subjected to the SWPS between $E_l = 0.6$ V and $E_u = 2.5$ V at $f = 5$ kHz during $t = 10$ s, a thick reddish-brown oxide layer is formed. This layer corresponds to a hydrated gold oxide having a macroscopic amorphous structure as is demonstrated by X-ray diffraction.

When the thick oxide layer is dehydrated by streaming dry nitrogen at room temperature over it, it becomes darker and its original volume is reduced to about one half. The thick oxide layer exhibits a dry-mud structure (Fig. 2). The potentiodynamic electroreduction profile run immediately after applying the SWPS

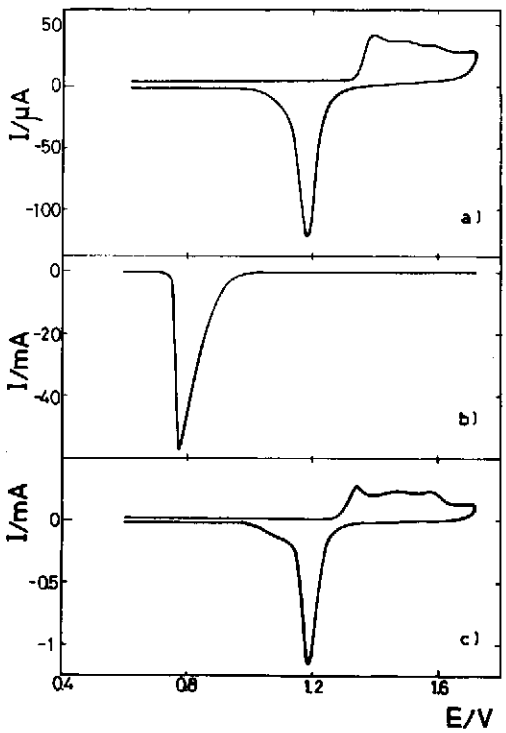

Fig. 1. Potentiodynamic *E/I* profiles run with 1 *M* $HClO_4$ at 30 °C. (a) Electropolished gold electrode after 5 min RTPS at 0.1 V/s (blank). (b) Electroreduction profile at 0.01 V/s immediately after the SWPS treatment ($E_u = 2.5$ V, $E_l = 0.6$ V, $f = 5$ kHz, $t = 10$ s). (c) Electroreduced gold after 5 min RTPS at 0.1 V/s.

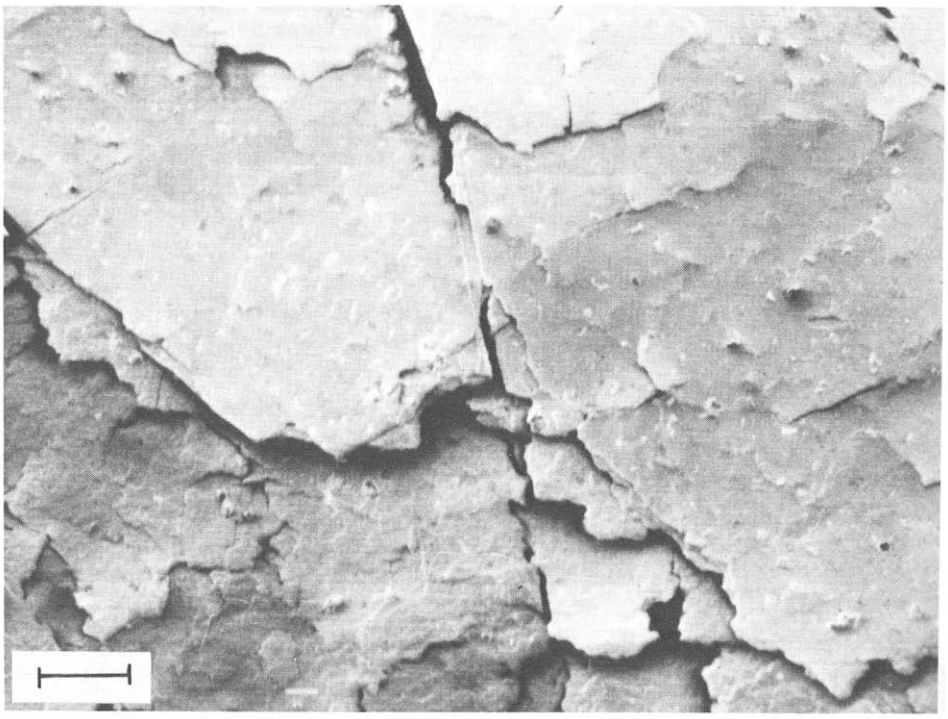

Fig. 2. SEM photograph of the thick gold oxide layer obtained after the SWPS treatment ($E_u = 2.7$ V, $E_l = 0.6$ V, $f = 5$ kHz, $t = 30$ s, 1 M $HClO_4$, 30 °C). Bar is 0.2 mm.

shows an asymmetric cathodic current peak at ca. 0.76 V (Fig. 1b) which corresponds to the electroreduction of the thick fresh oxide layer. In this case, the electroreduction charge is ca. 180 mC/cm^2. Once the thick oxide layer has been electroreduced, a net increase in the electrode surface area is observed (Fig. 1c). The corresponding RTPS voltammogram is close to the initial one (Fig. 1a), although the relative distribution of the various contributions related to the electroadsorption of oxygen in the complex anodic E/I profile has been considerably altered.

The relative actual increase in the real electrode area (R) is evaluated through the following relationship:

$$R = (Q_o)_a/(Q_o)_b \tag{1}$$

where Q_o denotes the electroreduction charge of the oxide layer formed during the anodic potential sweep up to 1.75 V before (b), and after (a), the SWPS treatment. For the sequence of E/I profiles depicted in Fig. 1, $R \simeq 10$.

The difference between the X-ray diffractograms (from 35° to 80°) of the base gold surface and that resulting after the electroreduction following the SWPS treatment is considerable (Fig. 3). The former shows a remarkable intensity increase of the peak related to the (220) plane (Fig. 3a) corresponding to a textured surface as

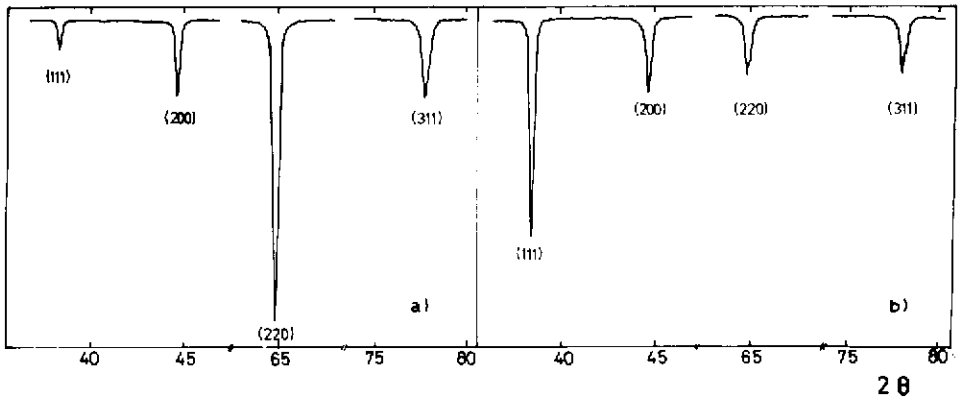

Fig. 3. X-ray diffractograms obtained with: (a) gold electrode without SWPS treatment; (b) electroreduced gold surface after the SWPS treatment ($E_u = 2.7$ V; $E_l = 0.6$ V; $f = 5$ kHz; $t = 30$ s; 1 M $HClO_4$, 30 °C).

a consequence of the rolling process of the base metal while the latter (Fig. 3b) presents a relative peak intensity distribution close to that corresponding to the gold standard. In this case, the scanning electron micrographs of the electroreduced gold

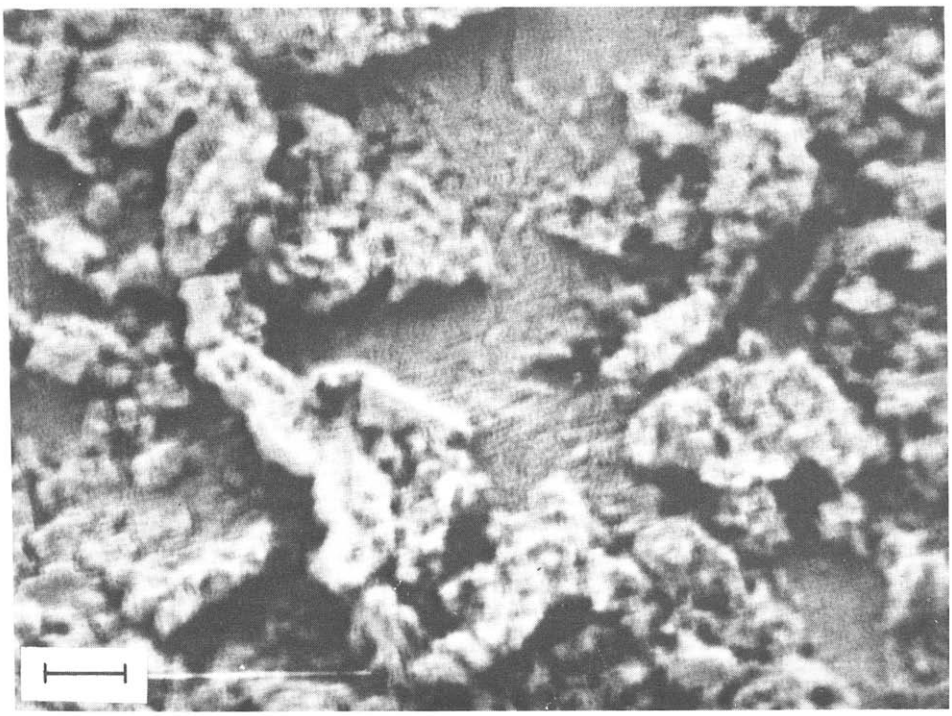

Fig. 4. SEM photograph of the electroreduced gold surface after the SWPS treatment ($E_u = 2.7$ V; $E_l = 0.6$ V, $f = 5$ kHz; $t = 30$ s, 1 M $HClO_4$, 30 °C). Bar is 0.02 mm.

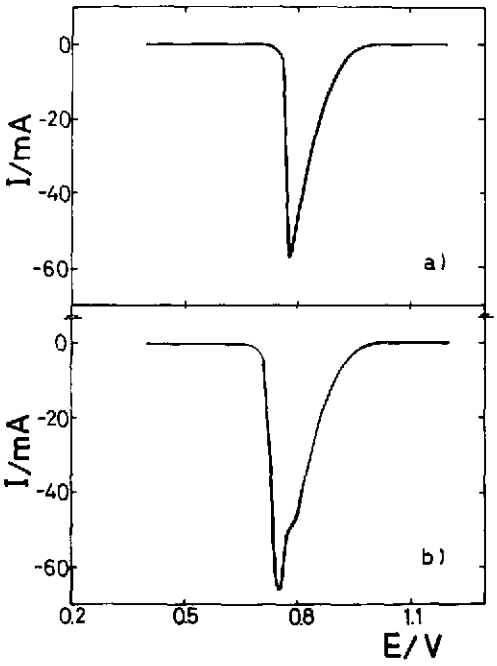

Fig. 5. Potentiodynamic E/I profiles at 0.01 V/s run immediately after the SWPS treatment ($E_l = 0.6$ V; $f = 5$ kHz, $t = 10$ s, 1 M $HClO_4$, 30 °C) at different E_u. (a) $E_u = 2.4$ V; (b) $E_u = 2.7$ V.

surface show a rough structure with vestiges of the original metal surface (Fig. 4).

Atomic absorption analysis of solution samples showed no evidence of gold ionic species in solution ($\leqslant 1$ ppm) when the gold electrodes were subjected to the SWPS for 2 h under the optimal conditions referred to further on. This result agreed with previously reported data obtained using RTPS techniques [9,15].

The electroreduction profiles run after the SWPS treatment are considerably dependent on E_u (Fig. 5). Thus, when $E_u < 2.5$ V, the E/I profile initiates at ca. 1.0 V with a continuously increasing cathodic current and once the peak current is attained a sharp current decrease to $I = 0$ is observed (Fig. 5a). This decrease can be attributed to the depletion of the oxide layer. On the other hand, when $E_u > 2.5$ V the electroreduction profiles exhibit an inflexion in the region preceding the current peak and at potentials more negative than the peak potential they approach a gaussian shape (Fig. 5b).

(2) Dependence of the electroreduction charge of the hydrated gold oxide on the characteristics of the SWPS

The electroreduction charge related to the thick gold oxide layer (Q_r) recorded after the SWPS treatment is taken as a measure of the relative actual increase in the real electrode area, R (Fig. 6).

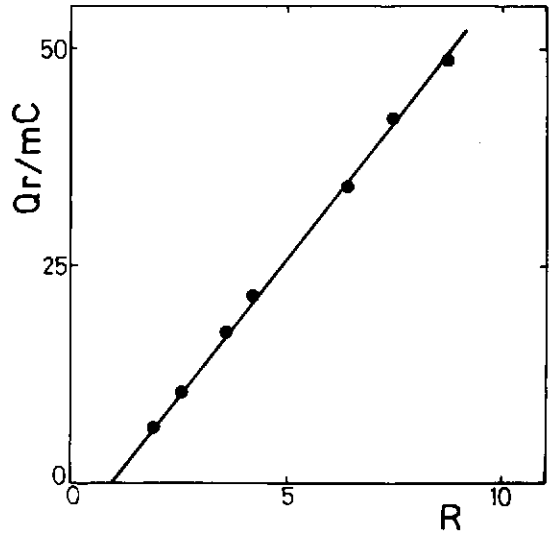

Fig. 6. Relationship between Q_r and R. SWPS characteristics: $E_u = 2.7$ V; $E_l = 0.6$ V; $f = 5$ kHz, 1 M $HClO_4$, 30 °C.

For constant E_l, f and t the electroreduction charge of the hydrated gold oxide depends on E_u (Fig. 7). The Q_r vs. E_u plot shows that q_r attains a maximum value at ca. 2.85 V when $E_l = 0.6$ V, $f = 5$ kHz and $t = 10$ s. Also, the Q_r vs. E_u plot shows a threshold potential at $E_u \simeq 2.1$ V beyond which the SWPS becomes effective in increasing the charge of the anodic oxide film. The value of E_u threshold potential

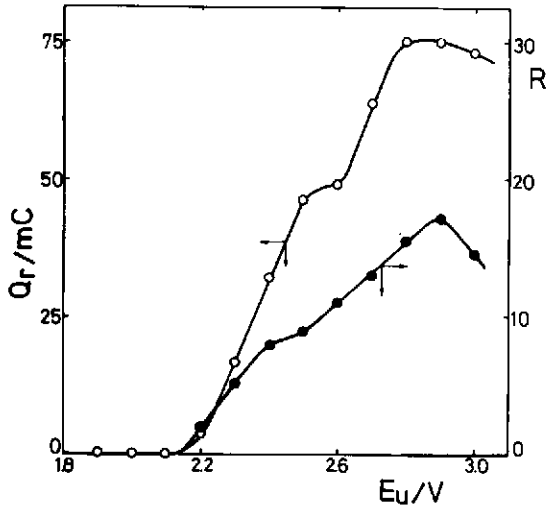

Fig. 7. Dependence of Q_r and R on E_u. SWPS characteristics: $E_l = 0.6$ V, $f = 5$ kHz, $t = 10$ s; $HClO_4$ 1 M, 30 °C.

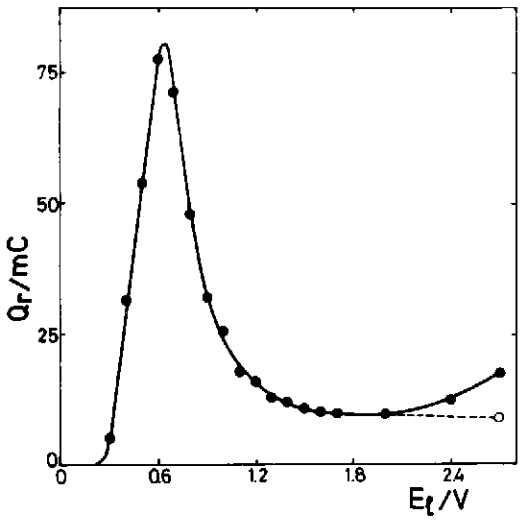

Fig. 8. Dependence of Q_r on E_l. SWPS characteristics: $E_u = 2.7$ V, $f = 5$ kHz, $t = 10$ s, 1 M $HClO_4$, 30 °C. The open circle corresponds to the potentiostatic condition at $E = 2.7$ V during 5 s.

for gold is very close to that already reported for platinum electrodes [14]. Furthermore, the Q_r vs. E_u plot presents an inflexion in the 2.5 V–2.6 V range. This fact correlates with the change in the electroreduction profiles of the hydrated oxide layer which takes place at $E_u = 2.5$ V. These results suggest that different oxide species are

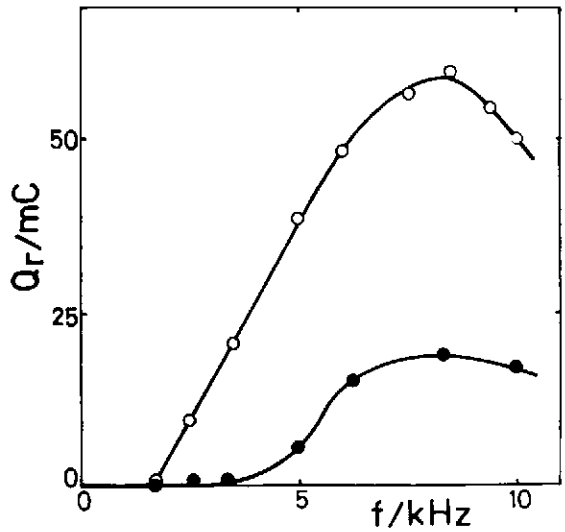

Fig. 9. Dependence of Q_r on f at different E_u. SWPS characteristics: $E_l = 0.5$ V, $t = 10$ s, 1 M $HClO_4$, 30 °C. (○) $E_u = 2.7$ V; (●) $E_u = 2.4$ V.

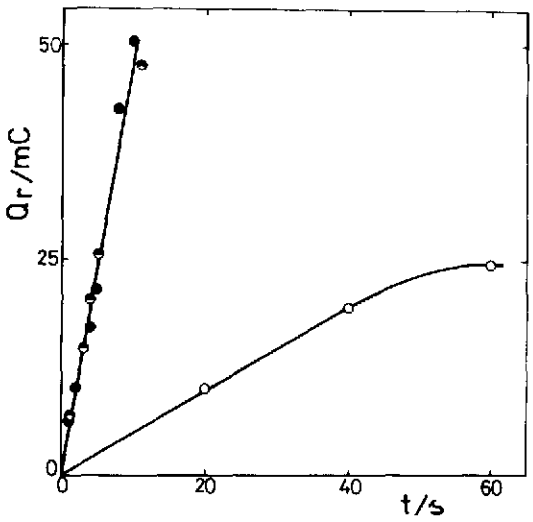

Fig. 10. Dependence of Q_r on t at different concentrations of perchloric acid (◓) 2 M, (●) 1 M, (○) 0.1 M. SWPS characteristics: $E_u = 2.7$ V, $E_l = 0.6$ V, $f = 5$ kHz, 20 °C.

produced when $E_u > 2.5$ V so that the electroreduction process involves a mixture of hydrated gold oxide species.

Under constant E_u, f and t, ($E_u = 2.7$ V, $f = 5$ kHz, $t = 10$ s), the dependence of Q_r on E_l shows a volcano relationship (Fig. 8), whose maximum appears at $E_l = 0.65$ V. Furthermore, the lowest value of E_l is ca. 0.2 V and the uppermost one is ca. 1.1 V. The latter coincides with the potential where the potentiodynamic electroreduction of the gold oxide monolayer is accomplished (Fig. 1).

For preset E_u, E_l and t values, the Q_r vs. f plot also exhibits a maximum Q_r value at 8.5 kHz (Fig. 9). The minimum frequency for the oxide layer formation is ca. 1.0 kHz, a value which is also close to that previously reported for platinum in the same electrolyte [14].

The amount of hydrated gold oxide produced by the SWPS treatment, as measured through the Q_r values, under constant E_u, E_l and f, increases linearly with t (Fig. 10). On the other hand, the rate of the oxide layer electroformation under preset conditions, increases with the electrolyte concentration to approach a limiting value estimated as 20 mC s^{-1} cm^{-2} (Fig. 10). Furthermore, the potential of the current peak related to the electroreduction of the hydrated gold oxide shifts towards the negative potential side with increasing t.

(3) Influence of the symmetry of the SWPS on the electrochemical characteristics of the anodic film

At constant E_u, E_l, f and t, the increase of Q_r depends on the symmetry of the SWPS, i.e., on both τ_l and τ_u. Thus, for $E_u = 2.7$ V, $E_l = 0.6$ V, $f = 4$ kHz, $t = 5$ s, Q_r

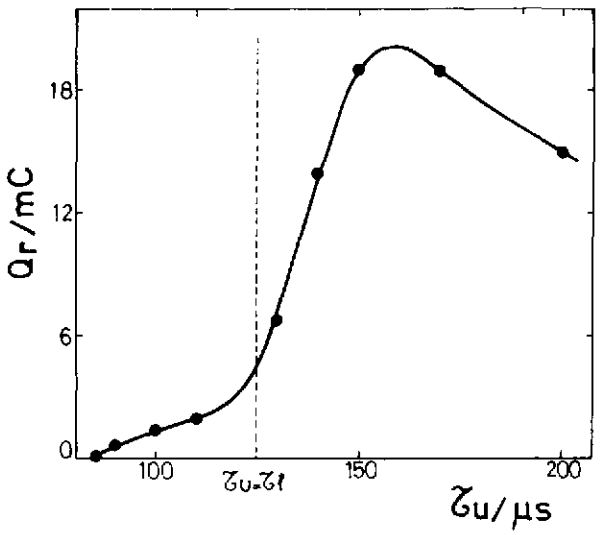

Fig. 11. Dependence of Q_r on τ_u at constant frequency. SWPS characteristics: $E_u = 2.7$ V, $E_l = 0.6$ V; $f = 4$ kHz, $t = 5$ s, 1 M $HClO_4$, 30 °C.

reaches a maximum at $\tau_u \simeq 160$ μs (Fig. 11). In this case, the value of Q_r is nearly four times that resulting when $\tau_u = \tau_l$. This result indicates that in this case, two counterbalancing effects determine the Q_r value. From one side, as τ_u becomes larger than 85 μs, the anodic layer is incompletely reduced during τ_l and a net oxide growth is then observed. On the other hand, when τ_u exceeds 160 μs, as the potentiostatic oxide growth conditions are gradually approached, Q_r decreases with the increase of τ_u. Therefore, a maximum is reached in the Q_r vs. τ_u plot.

DISCUSSION

When a polycrystalline gold electrode is subjected to the SWPS between E_u and E_l the metal surface changes alternately from a potential where a gold oxide layer is potentiostatically formed to another one in which the oxide layer is electroreduced at a constant potential. In this case, however, depending on the E_l value, the anodic layer is either partially or completely electroreduced. As deduced from the electroreduction voltammogram resulting after the SWPS (Fig. 5) the composition of the anodic oxide layer changes according to E_u.

It is already known that at potentials above 1.36 V Au_2O_3 can be formed [5] according to the following reaction:

$$2\ Au + 3\ H_2O = (Au_2O_3)_{mono} + 6\ H^+ + 6\ e^- \qquad (2)$$

At potentials below 2.0 V the growth of the thin oxide layer takes place according to a high field mechanism, as proposed by Lohrengel and Schultze [16]. When the potential exceeds 2.0 V the formation of thick layers was observed [9,16]. Therefore,

the anodic oxide layer should involve a compact, largely anhydrous, inner layer in contact with the metal surface which is covered by a thicker, porous hydrated outer layer in contact with the electrolyte solution. This duplex structure has already been proposed by Lohrengel and Schultze [16] and by Burke and McRann [9].

The efficiency of the oxide growth process under the SWPS is mainly characterized by three parameters, namely E_1, E_u and f and to a lesser extent by the electrolyte composition. As far as E_i is concerned, the value corresponding to the maximum efficiency is located in the potential range where the oxide monolayer has been completely electroreduced, as deduced from a direct comparison of Figs. 1 and 8.

Results show that both gold and platinum in the same solution exhibit the same threshold potential, $E_u = 2.1$ V, to achieve a macroscopic growth of the hydrated anodic oxide film. This coincidence suggests that the film growth above 2.1 V becomes a process which is apparently, to a great extent, independent of the electrode material. Such a fact can be explained through the formation of peroxide species, which in the case of platinum is related to the PtO_2/PtO_3 redox couple ($E° = 2.1$ V) [14]. For gold, peroxide species are detected when the potential is already in the vicinity of the potential where the O-monolayer electroadsorbed on gold is practically completed [5,17]. In both cases, these peroxide structures undergo either a partial chemical decomposition yielding oxygen or act as intermediates in ozone formation. The yield of the latter increases with the acid electrolyte concentration [17]. As a matter of fact, the onset of thick film growth on gold becomes appreciable above about 2 V in a potential region where a linear Tafel behaviour is observed for the oxygen evolution on gold [5,16,18].

From the lowest E_u value up to $E_u < 2.5$ V, there is a monotonous increase of Q_r with E_u and, in addition, in good agreement with previous results [19], the increase in Q_r occurs at a potential range where, according to bulk thermodynamics, only Au(III) species are stable [20]. Therefore, the anodic film growth at $E_u < 2.5$ V should involve hydrated Au_2O_3 phases. One possible formation of these amorphous phases is through the Au_2O_3 monolayer, according to:

$$Au_x(Au_2O_3)_{mono} + 3\ H_2O = Au_{x-2}(Au_2O_3)_{mono} + Au_2O_3 + 6\ H^+ + 6\ e^- \qquad (3)$$

Reaction (3) yields a sandwich like structure electrode of the type metal/oxide(I)/oxide(II). The existence of the monolayer is concluded from results shown in Fig. 12.

The Q_r/E_u plot also shows a small discontinuity in the 2.5 V–2.6 V range. This fact should be related to the appearance of an inflexion in the electroreduction profile when $E_u > 2.5$ V, and it indicates a kinetic change in the electrochemical process. This potential range coincides with the thermodynamic potential for the electroformation of Au(IV) species, since:

$$Au_2O_3 + H_2O = 2\ AuO_2 + 2\ H^+ + 2\ e^- \qquad E° \simeq 2.5\ V \qquad (4)$$

Consequently, the composition of the anodic film when E_u exceeds 2.5 V is probably a mixture of Au(III) and Au(IV) hydrated oxide species. Furthermore, the two linear regions resulting from the Q_r vs. log τ_u plot suggest the existence of two different

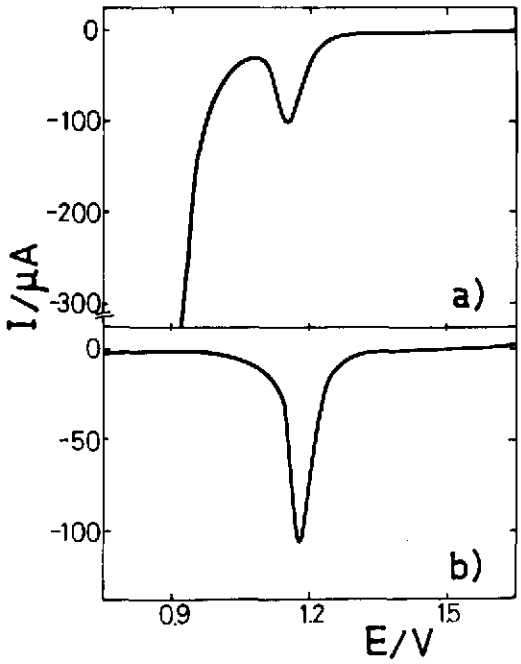

Fig. 12. Potentiodynamic E/I profiles run with 1 M $HClO_4$ at 30 °C. (a) Electroreduction profile at 0.01 V/s immediately after the SWPS treatment ($E_u = 2.4$ V; $E_l = 0.5$ V; $f = 4$ kHz, $t = 10$ s). (b) Electroreduced gold after 5 min RTPS at 0.1 V/s.

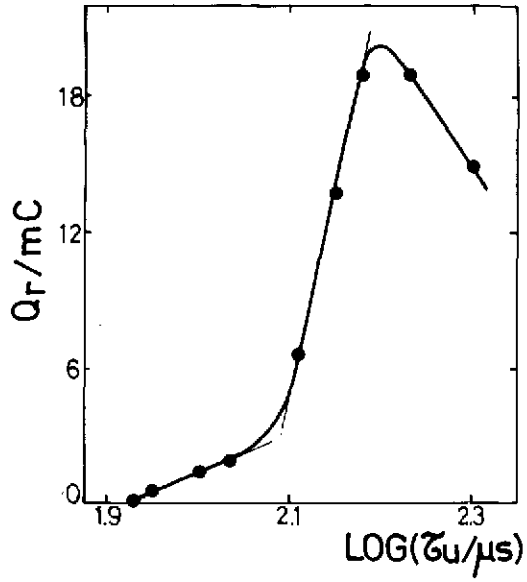

Fig. 13. Q_r vs. $\log \tau_u$ plot derived from the data indicated in Fig. 11.

kinetics in the oxide growth (Fig. 13). As a matter of fact, the formation of Au(IV) species from $Au(OH)_3$ becomes possible when the equilibrium potential of the reaction

$$Au(OH)_3 = AuO_2 + H_2O + H^+ + e^- \qquad E^\circ = 2.305 \text{ V} \tag{5}$$

is exceeded, but there is no clear evidence that in the present case at this potential Au(IV) species are already formed.

The rate of anodic film growth depends on the electrolyte concentration as it arises from the change of the slope derived from the Q_r vs. t plots (Fig. 9) at different concentrations. The value of the slope depends on the specific conductivity of the electrolyte solution.

The potentiodynamic electroreduction of the anodic film resulting after the SWPS produces a remarkable increase in the real electrode area and structural changes in the electrode surface which exhibits a polycrystalline structure with a random grain distribution without any preferential orientation of grains.

It should be noticed that the E_u threshold potential values both for gold and platinum in 1 M $HClO_4$ are practically the same ($E_u \simeq 2.1$ V). This, in principle, suggests that, unless a fortuitous coincidence, a common redox reaction in solution (e.g., $O_2 + H_2O = O_3 + 2\ H^+ + 2\ e^-$; $E^\circ = 2.07$ V) becomes potential determining in both cases. In this respect one may relate this reaction to the formation of peroxide structures during the oxide growth. However, this may be a necessary but not sufficient condition because it does not explain the great difference in rate of oxide growth under SWPS or potentiostatic conditions. The greatest efficiency of SWPS is associated with E_1 values in the potential range where M–O bonds are broken and M–M bonds are formed. Both processes imply a relaxation and reaccommodation of metal atoms at the reaction surface as represented in the following sequence:

$$\text{oxide layer} \overset{(H^+ + e^-)}{\rightarrow} M^* \tag{6}$$

$$M^* \overset{v_r}{\rightarrow} M \tag{7}$$

During the electrooxidation half-cycle the formation of oxide layer takes place according to:

$$M^* \overset{-(H^+ + e^-)}{\rightarrow} \text{oxide layer} \tag{8}$$

This means that reaction (6) yields a non-equilibrium metal atom which rearranges into a stable site in the lattice at the rate v_r. Therefore, at low frequencies, only M is formed and the electrooxidation of the base metal is hindered. Otherwise, at large frequencies the probability that reaction (8) may occur decreases. In terms of the simplified reaction model, the common threshold frequency of SWPS corresponding to the initiation of oxide growth for both gold and platinum can be related to the half-life time ($t_{1/2}$) of M* atoms. For gold, $t_{1/2} \simeq 1 \times 10^{-3}$ s, in good agreement

with that of the $Au(OH)_{ad}$ species previously determined in acid electrolytes [21] and for platinum, $t_{1/2} \simeq 2 \times 10^{-3}$ s, which also corresponds to the relaxation time of the $Pt(OH)_{ad}$ species [22].

Therefore, the rate of metal atom reaccomodation at the interface appears to determine the efficiency of the SWPS treatment and the optimal frequency range of SWPS results from a compromise between the rate of the metal atom reaccomodation reaction following the electroreduction half-cycle and the rate of non-equilibrium metal atom electrooxidation.

ACKNOWLEDGEMENTS

INIFTA is sponsored by the Consejo Nacional de Investigaciones Científicas y Técnicas, the Universidad Nacional de La Plata and the Comisión de Investigaciones Científicas (Provincia de Buenos Aires).

This work was partially sponsored by the Organization of the American States.

REFERENCES

1 J.P. Hoare, Electrochim. Acta, 9 (1964) 1289.
2 L.D. Burke and D.P. Whelan, J. Electroanal. Chem., 124 (1981) 333.
3 L.D. Burke and E.J.M. O'Sullivan, J. Electroanal. Chem., 117 (1981) 155.
4 H.A. Laitinen and M.S. Chao, J. Electrochem. Soc., 108 (1961) 726.
5 S. Barnartt, J. Electrochem. Soc., 106 (1959) 722.
6 J.O.E. McIntyre, W.F. Peck and S. Nakahara, J. Electrochem. Soc., 127 (1980) 1264.
7 S. Shibata, Electrochim. Acta, 17 (1972) 395.
8 R. Córdova O., M.E. Martins and A.J. Arvía, J. Electrochem. Soc., 126 (1979) 1172.
9 L.D. Burke and M. McRann, J. Electroanal. Chem., 125 (1981) 387.
10 B.E. Conway, M. Angerstein-Kozlowska and L.H. Labiberté, J. Electrochem. Soc., 121 (1974) 1596.
11 J. Horkans, B.D. Cahan and E. Yeager, Surf. Sci., 46 (1974) 1.
12 Yu.Ya. Vinnikov, V.A. Shepelin and V.I. Veselovskii, Elektrokhimiya, 8 (1972) 1229.
13 R. Córdova O., M.E. Martins and A.J. Arvía, Electrochim. Acta, 25 (1980) 453.
14 A.C. Chialvo, W.E. Triaca and A.J. Arvía, J. Electroanal. Chem., 146 (1983) 93.
15 D.A.J. Rand and R. Woods, J. Electroanal. Chem., 35 (1972) 209.
16 M.M. Lohrengel and J.W. Schultze, Electrochim. Acta, 21 (1976) 957.
17 T.R. Beck and R.W. Moulton, J. Electrochem. Soc., 103 (1956) 247.
18 J.J. MacDonald and B.E. Conway, Proc. R. Soc., A269 (1962) 419.
19 T. Dickinson, A.F. Povey and P.M.A. Sherwood, J. Chem. Soc. Faraday Trans. I, 71 (1975) 298.
20 J. Van Muylder and M. Pourbaix in M. Pourbaix (Ed.), Atlas of Electrochemical Equilibria in Aqueous Solutions, Pergamon Press, Oxford, 1966.
21 C.M. Ferro, A.J. Calandra and A.J. Arvía, J. Electroanal. Chem., 59 (1975) 239.
22 B.E. Conway, H. Angerstein-Kozlowska, F.C. Ho, J. Klinger, B. MacDougall and S. Gottesfeld, Faraday Discuss. Chem. Soc., 56 (1973) 210.